BBC RD 1979/11

RESEARCH DEPARTMENT REPORT

The limitation of resolution of a colour television display by the sampling characteristics of the shadow mask

C.R.G. Reed, M.A.(Oxon.), C.Eng., M.I.E.E.

Research Department, Engineering Division
THE BRITISH BROADCASTING CORPORATION June 1979

BBC RD 1979/11
UDC 621.397.331.244.1
621.391.837.3

THE LIMITATION OF RESOLUTION OF A COLOUR TELEVISION DISPLAY BY THE SAMPLING CHARACTERISTICS OF THE SHADOW MASK

C.R.G. Reed, M.A.(Oxon.), C.Eng., M.I.E.E.

Summary

The resolution of colour-television displays on shadow-mask tubes, either of the traditional type in which the guns are grouped in delta-formation around the tube axis or the more recent type in which they lie in a horizontal plane (known as in-line-gun tubes) can be limited by the sampling action of the mask structure. This Report considers the patterning produced on large uniform areas and the resolution of single edges and repetitive detail, taking account of the line structure of the raster and the apertures in the shadow mask but assuming that the information is stationary.

Issued under the authority of

Head of Research Department

Research Department, Engineering Division,
BRITISH BROADCASTING CORPORATION

June 1979

(PH-204)

THE LIMITATION OF RESOLUTION OF A COLOUR TELEVISION DISPLAY BY THE SAMPLING CHARACTERISTIC OF THE SHADOW MASK

Section Title Page

Summary .... Title Page

1. Introduction 1

2. The apertures in a shadow mask 1

3. Patterns visible in large areas of uniform brightness and colour 1

4. The resolution of the edge of a large area 2

5. Sampling and signal patterns that vary repetitively in the line direction but do not vary in the field direction. 4

5.1 The theory of sampling in the line direction 4
5.2 A line-sweep waveform displayed on an in-line-gun tube 7

6. Two-dimensional sampling 7

6.1 Representation of a spatial frequency 7
6.2 Aperture arrays in the shadow mask 9
6.3 The sampling process 9
6.4 A line-sweep signal displayed on a delta-gun tube 9
  6.4.1 The display 9
  6.4.2 Sampling in the line direction only 9
  6.4.3 Sampling by the mask and the raster in the vertical direction only. 10
  6.4.4 Sampling by the shadow mask in an oblique direction 11

7. Reproduction of a hyperbolic zone plate test pattern 12

7.1 The test pattern 12
7.2 The hyperbolic zone plate test pattern displayed on an in-line-gun tube 13
  7.2.1 The display 13
  7.2.2 The moiré patterns 13
7.3 The hyperbolic zone plate test pattern displayed on a delta-gun tube 14
  7.3.1 The display 14
  7.3.2 The moiré patterns 14

8. Conclusions 16

9. References 16

Section Title Page

10. Appendix 17

10.1 Introduction 17
10.2 Spectral components 17
10.3 One-dimensional sampling 18
10.4 Two-dimensional sampling 19
10.5 The sampling effects of a shadow mask. 19

THE LIMITATION OF RESOLUTION OF A COLOUR TELEVISION DISPLAY BY THE SAMPLING CHARACTERISTIC OF THE SHADOW MASK

C.R.G. Reed, M.A.(Oxon.), C.Eng., M.I.E.E.

1. Introduction

The resolution of both monochrome and colour television tubes is limited by the finite size of the scanning spot, flare in the faceplate and the line structure of the raster. The shadow mask of a colour tube imposes further limitations on resolution, both by itself and in combination with the raster. Purity and convergence errors also degrade the resolution, both these effects will be ignored in this Report.

Calculations related to patterning on the display involve both physical dimensions, such as the sampling or display pattern wavelength, and electrical terms such as the frequency f. For convenience, both of these will be expressed throughout this Report in terms of electrical frequency in MHz, the equivalent frequency of a pattern with wavelength λ, no matter whether it is vertical, horizontal or oblique, being taken as that signal frequency which, applied during every line in the same timing relationship relative to the sync pulses, would produce a pattern of vertical bars with wavelength λ. Taking the screen width as W and the active line time as 52 μs, $f = W/52\lambda$.

2. The apertures in a shadow mask

In the traditional form of shadow mask tube the electron guns are grouped round the tube axis, with the Blue gun at the top. This is known as a delta-gun arrangement, from the layout in a cross-section of the tube neck. The pattern of holes in the shadow-mask and the positions of the phosphor dots are shown, in idealised form, in Fig. 1.

More recently, tubes have been developed in which the electron guns lie in a horizontal plane[1], and this is known as an in-line-gun arrangement because of its layout in the tube cross-section. The associated mask structure and phosphor areas are shown, in idealised form, in Fig. 2.

The main advantages of the in-line-gun tube, which result from its symmetry about the plane of the guns, are the simplifications of the problems of purity and convergence so that dynamic convergence correction is only required on the larger tubes with wide-angle deflection.

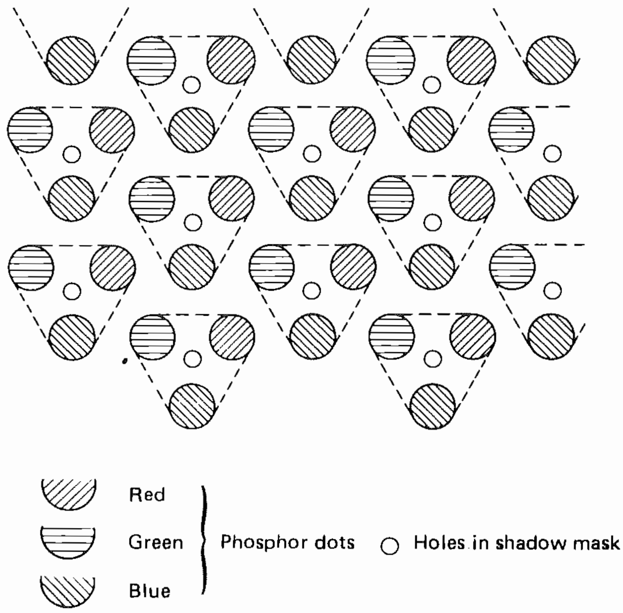

Fig. 1 - Phosphor triads near the centre of the screen of a delta-gun shadow-mask tube.

The use of a slotted mask, with thin horizontal bridges across the slots to give rigidity, results in a display with virtually no sampling effects in the vertical direction apart from those inherent in the structure of the scanning raster. The delta arrangement involves sampling processes in all directions, but has the advantage that in the horizontal direction the apertures of one row are interlaced between the apertures of the rows above and below. When tubes of the two types, with masks involving similar mechanical tolerances, are compared the delta-gun aperture mask has significantly better horizontal resolution.

3. Patterns visible in large areas of uniform brightness and colour.

In both types of tube the raster structure and the layout of the phosphor areas are visible on close inspection.

In a delta-gun tube two effects can be seen, resulting from the interaction between the line structure and the shadow mask pattern[2].

(a) If the beam focus produces a scanning spot with a small vertical dimension and the spacing

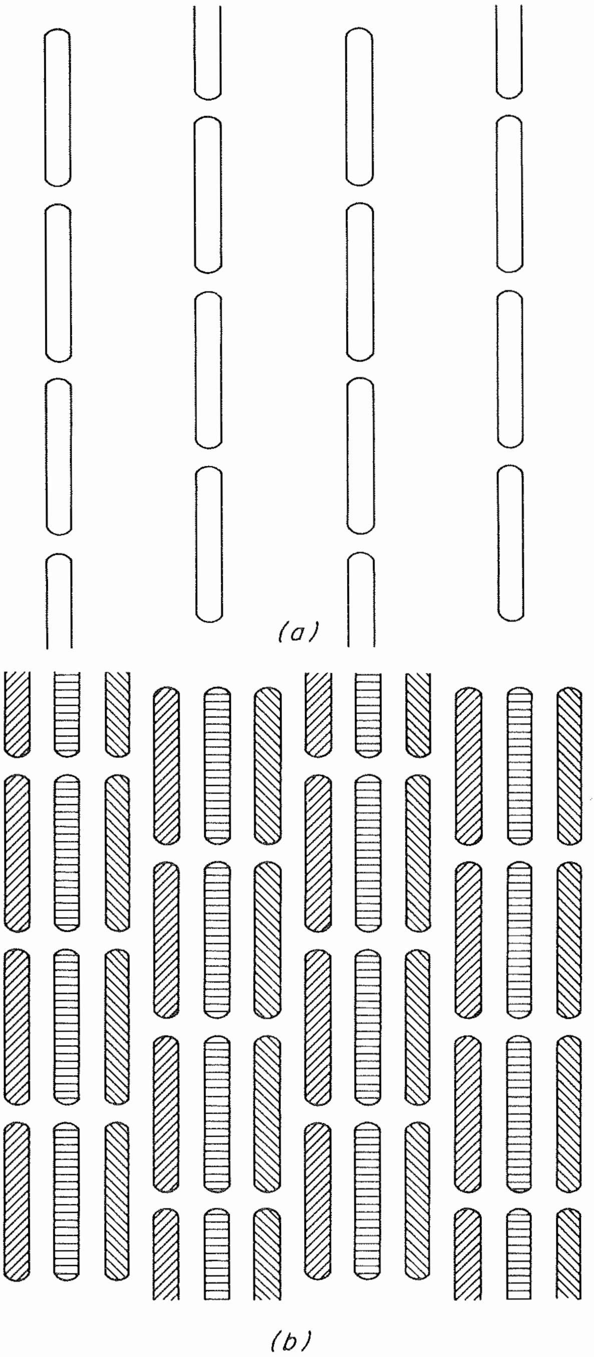

Fig. 2 - The shadow-mask tube with in-line guns

(a) Slots in the shadow-mask (b) Phosphor stripes

▨ Red ▤ Green ▧ Blue

between picture lines of a scan is slightly different from an integral multiple of the spacing between horizontal rows of apertures, there will be bands of display area in which the scan lines pass near the centres of the apertures separated by darker bands in which the scan lines only pass over the edges of the apertures.

(b) If, in the condition described above, the picture line spacing is approximately twice the distance between horizontal rows of apertures the lines of one bright band excite only half of the columns of phosphor dots and the adjacent bright bands excite the interlaced columns of phosphor. This effect is usually only visible on close inspection.

The visibility of these patterns, particularly of the fine detail, depends on the sharpness of focus of the scanning beams. An example will be considered in Section 6.4.3.

4. The resolution of the edge of a large area

If the edge of a large area is nearly vertical the resolution is controlled by the shadow mask and, because of the interlacing effect noted in Section 2 is significantly better for a delta-gun tube than for a corresponding in-line-gun tube.

A representative in-line-gun tube with a 56 cm (22 in) screen has a picture width of 444 mm and a slot spacing 0.8 mm. The resulting frequency of sampling by the shadow mask in the horizontal direction, without overscan, is 10.67 MHz. The corresponding delta-gun tube has a spacing 0.68 mm between apertures, measured vertically or diagonally. The horizontal sampling frequency, allowing for the effect of the interlace is 14.5 MHz.

Fig. 3 shows the sampling by the mask of an in-line-gun tube of signals with two waveforms, one having a transition with the same shape as the rise of a 2—*T* pulse, i.e. half a cycle of a 2.5 MHz sine wave, the other being the response of a 5.5 MHz sharp-cut filter to a rapid transition. It is clear that although the sampling gives a fairly good representation of the position of the transition it fails to define its shape, particularly for the more rapid waveform.

The corresponding sampling effects in a delta-gun tube are shown in Fig. 4., the dashed lines showing the interlace on successive horizontal rows of apertures. The closer spacing of the samples gives better resolution of the transitions than an in-line-gun tube, but the acceptability of either for a particular application can only be decided by subjective tests.

When the edge of the area is slightly inclined to the vertical, the reproduction tends to be stepped, particularly with an in-line-gun tube, in the same way as the reproduction of a near horizontal edge is stepped by the line structure.

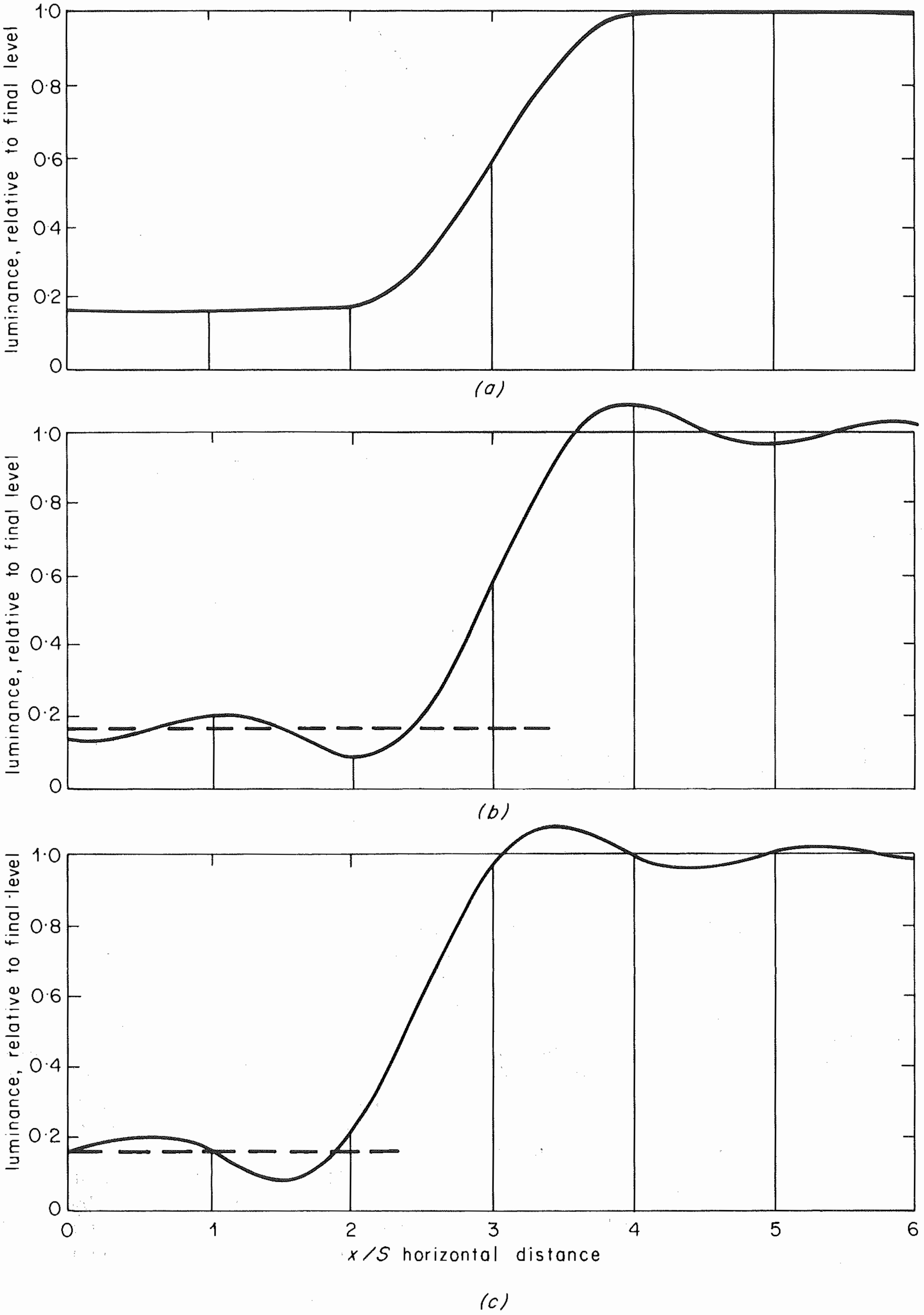

Fig. 3 - Sampling of a transition by an in-line-gun tube with horizontal sampling distance S.

(a) a 2-T transition

(b) a rapid transition modified by a 5.5 MHz filter.

(c) as (b), but in a different time relationship.

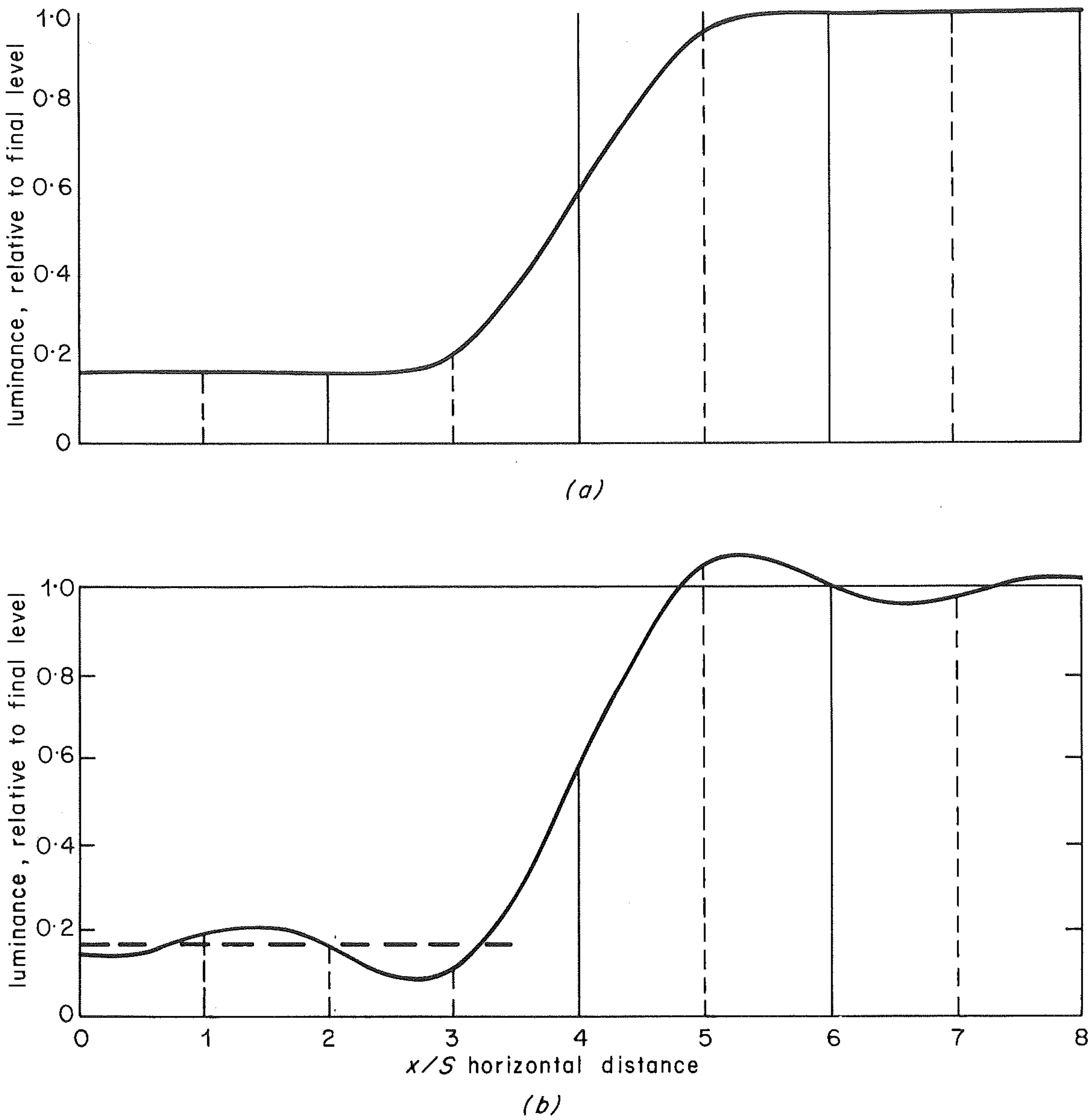

Fig. 4 - Sampling of a transition by a delta-gun tube with horizontal sampling distance S.,
(alternate samples are shown dashed to emphasise that they are produced by the interlacing columns of apertures)
(a) a 2-*T* transition.
(b) a rapid transition modified by a 5.5 MHz filter.

5. Sampling and signal patterns that vary repetitively in the line direction but do not vary in the field direction.

5.1 The theory of sampling in the line direction

The simplest condition is the sampling by the mask of an in-line-gun tube of a repetitive vertical-bar pattern, produced by a signal waveform that is the same for all lines (assuming a perfect scanned raster) and containing a repetition of cycles each of which corresponds to one bar of the pattern. If two of the beams could be switched off, the shadow mask removed and the phosphor of the appropriate colour made uniform over the scanned area, the luminance of the display would vary continuously with the horizontal displacement x and could be represented by the function $v\ (x)$. If this display is repetitive with wavelength λ mm and equivalent electrical frequency $f = W/52\ \lambda$ MHz (Sect. 1), it can be thought of as part of a repetitive pattern extending infinitely far to either side of the screen. This can be represented by a mean component a_0 and a set of sinusoidal components at frequencies equal to f and its harmonics.

The effects of the shadow mask with all three guns operating under idealised conditions, including perfect convergence and purity, are shown in Fig. 5 for six positions selected out of the continuous scan process. The horizontal scale has been exaggerated to show the detail of the sampling.

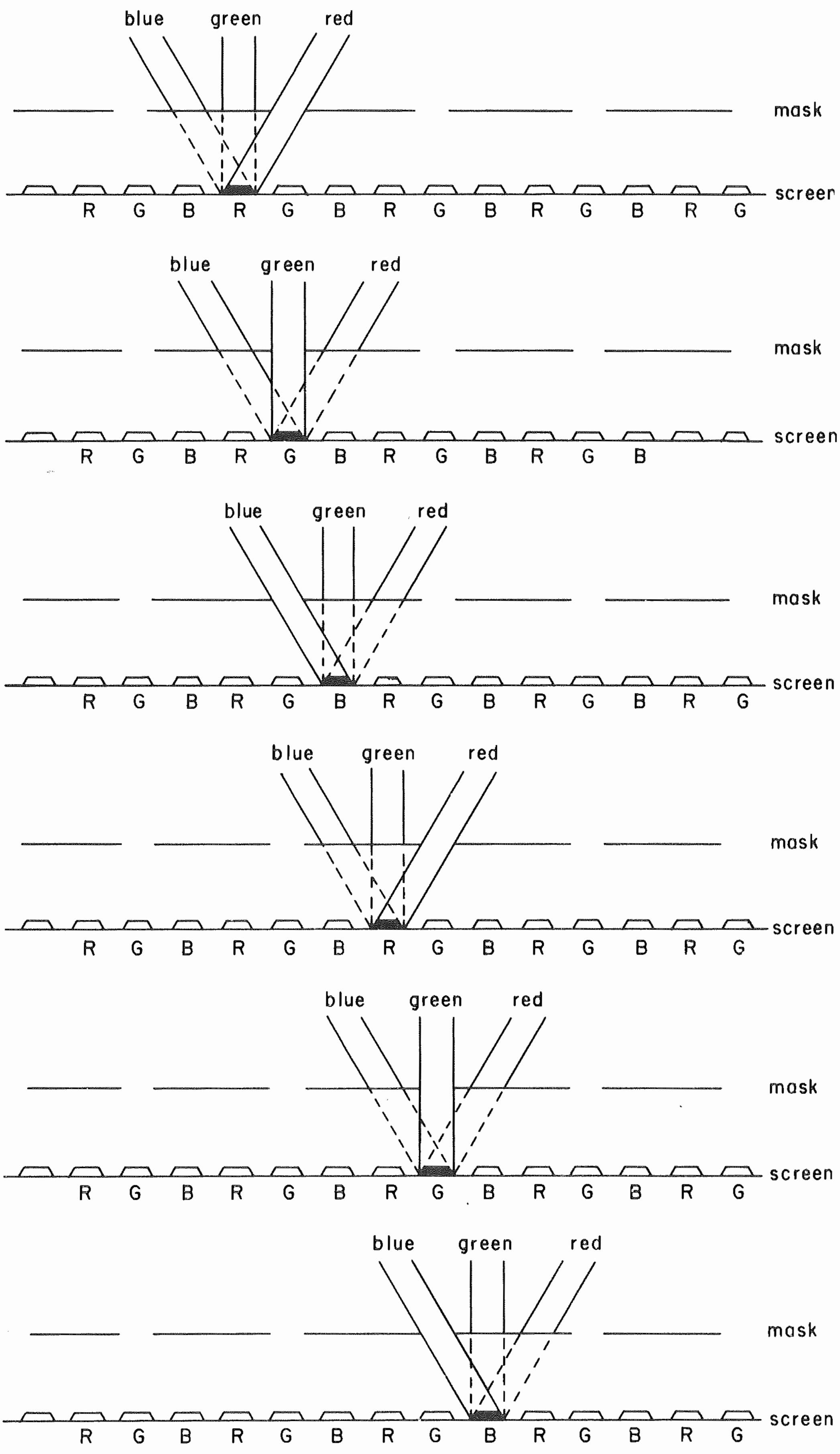

Fig. 5 - The sampling process of an in-line-gun tube.
(the horizontal scale has been greatly exaggerated)

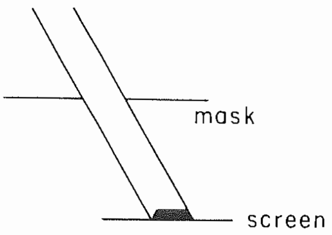

An electron beam passing through an aperture in the mask and exciting a phosphor area

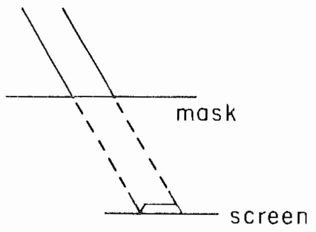

An electron beam obstructed by the mask and NOT exciting a phosphor area

The sampling process imposed by the mask on one of the primary-colour displays can be represented by a continuous function $s(x)$ which varies across the display and is such that the resulting luminance $i(x)$ is the product of $s(x)$ and $v(x)$

i.e. $$i(x) = s(x) \,.\, v(x)$$

A sampling process that is repetitive at a interval S mm, i.e. with equivalent electrical frequency $p = W/52S$ MHz, can also be thought of as part of an infinite repetition and represented by the sum of a mean component b_0 and sinusoidal components with frequencies equal to p and its harmonics.

The spectrum of $i(x)$ has two types of component

(i) The components of $v(x)$ multiplied by b_0, i.e. the original unsampled display attenuated by the mean transmission of the mask

(ii) the components of $v(x)$ multiplied by the sinusoidal components of the sampling pattern. The resulting spectrum consists of the sinusoidal components of $s(x)$, each multiplied by a_0 and accompanied by upper and lower sidebands proportional to the components of $v(x)$. The components of the spectrum thus have frequencies $f_m = (mp + nf)$ where m and n are integers (this is a similar process to amplitude modulation).

When the spectrum of $v(x)$ is restricted so that the frequency of its highest component is less than $p/2$ the spectrum after sampling is as shown in Fig. 6., but if the bandwidth of $v(x)$ is greater than $p/2$ the groups of sidebands overlap. In an electrical sampling system the original signal is recovered by using a low-pass filter to reject the sidebands of the a.c. components of the sampling waveform. This cannot be achieved if the groups of components overlap, and the unwanted parts of the spectrum left after low-pass filtering are known as 'alias' components. The sampling process of the display system is slightly different in that it does not contain an optical equivalent of the sharp-cut filter, so it is only the eye that attenuates the unwanted components in the perceived signal.

In some circumstances the luminance pattern $v(x)$ contains components at frequencies comparable to p or its harmonics, produced by non-linearity of the luminance/drive voltage characteristic of the tube. The frequency of the alias component, $f_m = (mp - nf)$, is then low and the corresponding pattern on the display is a coarse moiré pattern.

The sampling process will be considered in more detail in the Appendix where it will be shown (Section 10.3) that if the sampling pattern $s(x)$ is displaced bodily so that the fundamental component changes in phase by ψ and the luminance pattern $v(x)$ is displaced so that the phase of its fundamental is displaced by ϕ then the components after sampling at frequencies $(mp + nf)$ are shifted in phase by $(m\psi + n\phi)$. From Fig. 5 it is clear that, under conditions of perfect convergence, the phases of sampling of the three colours are spaced by 120°, so the phases of any moiré patterns are spaced by (m x 120°). This displacement of the three colours reduces the visibility of a moiré pattern resulting from a low-saturation signal compared with that produced by a signal in one of the primary colours, particularly if it is Green.

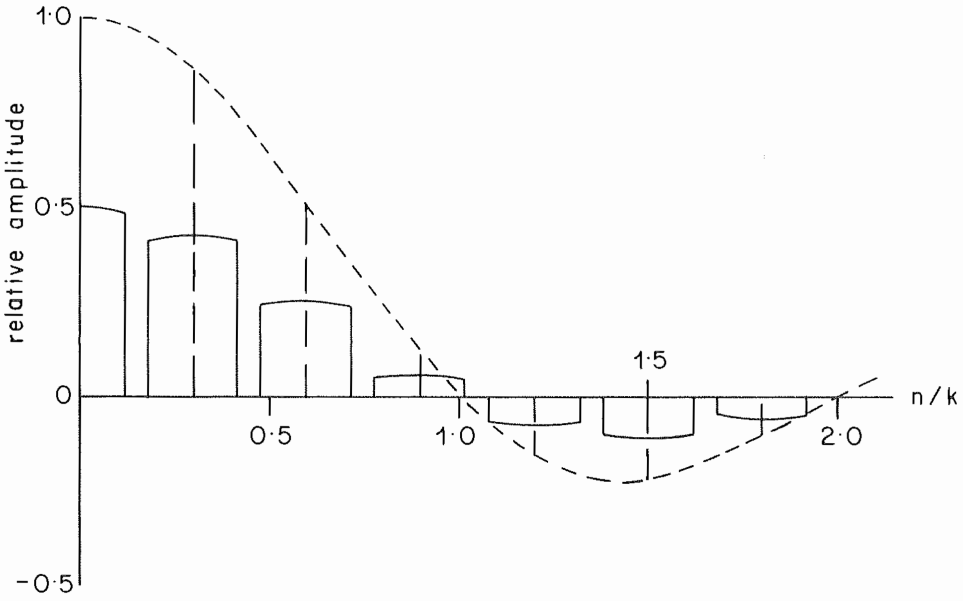

Fig. 6
Spectra involved in one-dimensional sampling

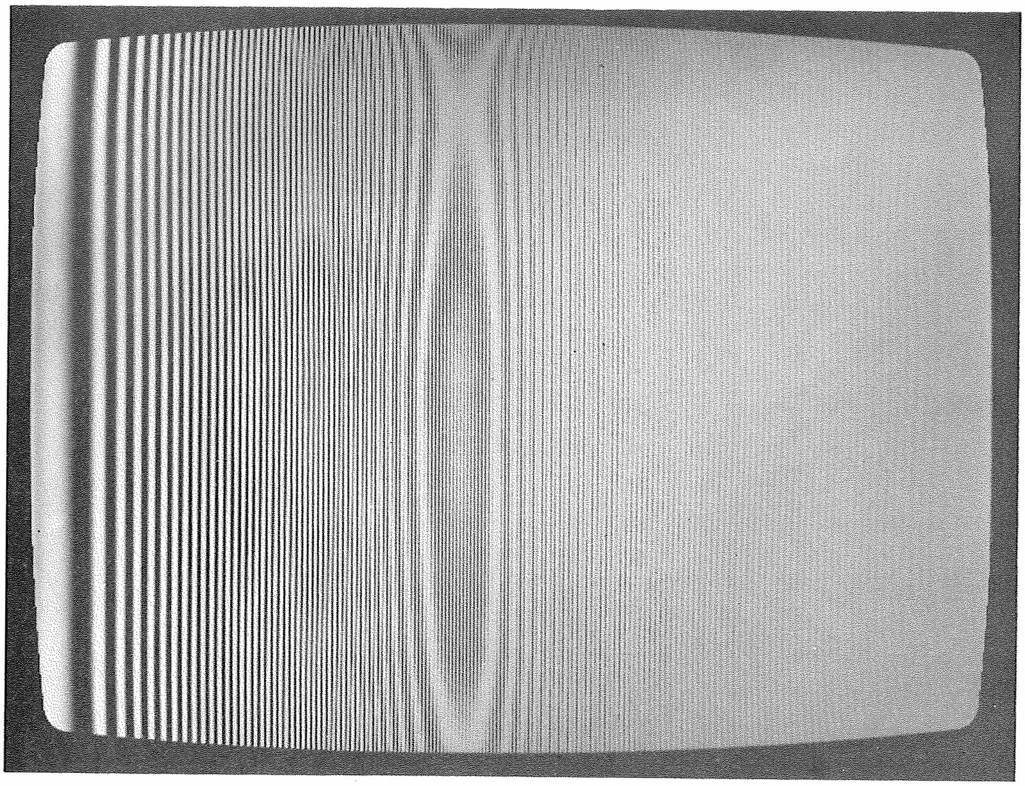

Fig. 7
Line-sweep waveform displayed on an in-line-gun tube
(Green phosphor only)

5.2 A line-sweep waveform displayed on an in-line-gun tube

A useful test signal is a line-sweep waveform, i.e. one consisting of a d.c. component and a sinusoidal component that starts on each line in a pre-determined phase and varies smoothly in frequency from the start to the end of the line. If this is repeated regularly at line frequency the display consists of vertical bars with smoothly-varying wavelength.

Any small part of this display can be treated as though it were part of a larger display with a constant frequency.

Fig. 7 shows such a display on a 56 cm. (22 in) in-line-gun tube with the Green gun active and the other two guns switched off. For this tube the screen width is 444 mm and the mask aperture wavelength 0.8 mm so the equivalent sampling frequency of the mask is $p = (444/52 \times 0.8) = 10.67$ MHz.

The sweep waveform frequency, f, increases from left to right between approximately 0.5 and 10 MHz. The alias component with frequency $(p - f)$, which increases from right to left, is seen towards the right-hand side of the display. Because of the non-linear characteristics of the tube, moiré patterns can be seen centred on the positions for which $(p - 2f) = 0$ and $(p - 3f) = 0$, i.e. $f = 10.67/2 = 5.34$ MHz and $f = 10.67/3 = 3.56$ MHz.

On a perfect display the moiré patterns would consist of vertical bars. However there are inevitably small variations over the picture of the phasing of the sinusoidal sweep, of the regularity of the line scan and of the uniformity of the shadow mask. These produce corresponding phase-shifts of the moiré patterns (cf, the last paragraph of Section 5.1). For example, a local distortion of the mask that displaces the apertures by 0.4 mm represents a phase reversal of the sampling and therefore of the moiré pattern; the same displacement of the 5.34 MHz component of the video signal represents a quarter-wave change of the fundamental and a phase reversal of the second harmonic, again reversing the phase of the moire pattern. Effects of this type are seen in Fig. 7 as the distortion of vertical moiré bars into closed loops.

6. Two-dimensional sampling

6.1 Representation of a spatial frequency

In Section 5 the displayed pattern and the sampling process each varied in the x – direction but not in the y – direction. This Section will deal with the more general condition in which the directions of the pattern and of the sampling process are inclined to one another.

The wavelength of a pattern is measured as

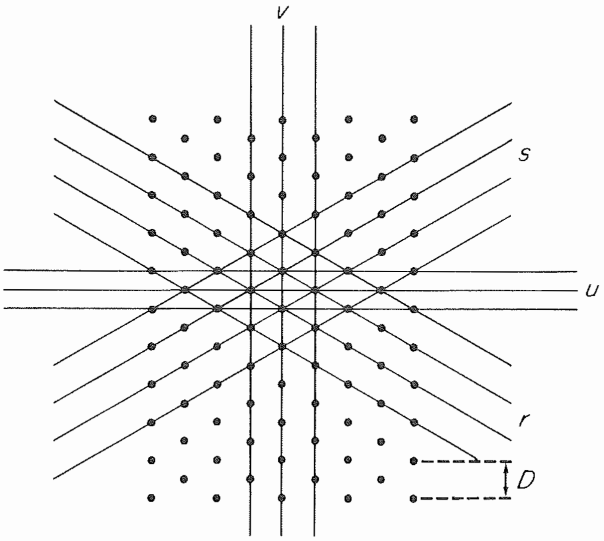

(a)

Fig. 8 - The apertures in the shadow-mask of a delta gun tube

(a) the four principle directions in which the apertures may be grouped into arrays

(b) vector representation of the spatial frequencies of the arrays

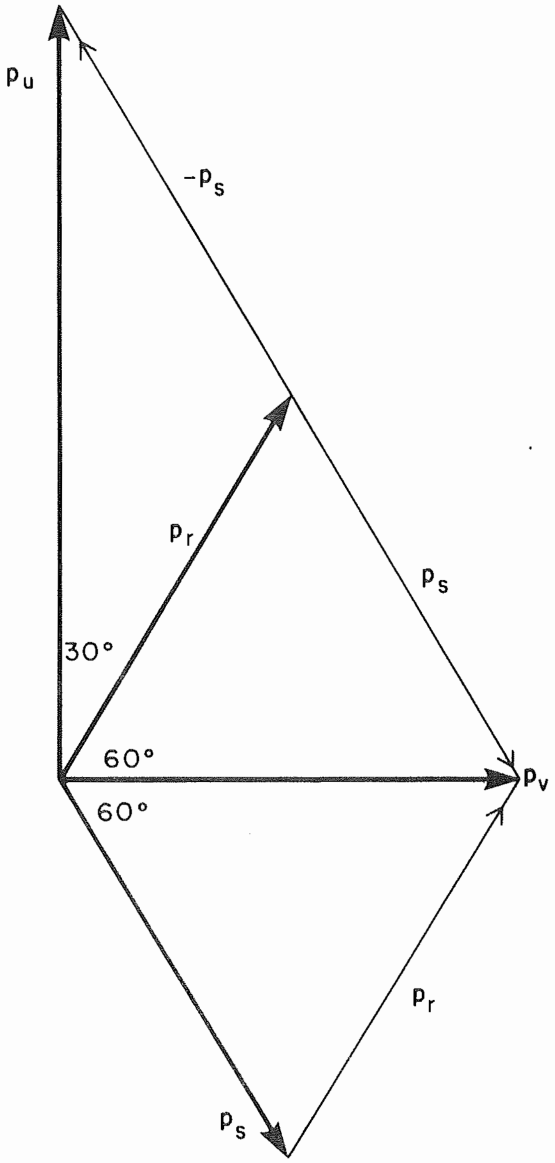

(b)

the shortest distance from one wave crest to the next, and is at right-angles to the crest and trough lines of the pattern. It is often convenient to represent the spatial frequency of the fundamental component of a stationary pattern by a vector whose length is proportional to the spatial frequency and whose direction is that in which the wavelength is measured. The harmonics are represented by vectors in the same direction whose length are integral multiples of this fundamental vector. The sense of the vector has no significance in this application – it may be reversed without changing its meaning, analogous to the absence of a sense of positive and negative directions on anything more than a completely arbitrary basis when considering a stationary sinusoidal wave pattern.

A vector is a representation of a quantity, in this application the spatial frequency of a pattern, in magnitude and direction; it does not represent in any way the amplitude or phase of the signal producing the pattern. This is totally distinct from a line in a phase diagram of a.c. circuit theory which represents the amplitude and phase of a signal but not the frequency or the direction of the resulting pattern.

It is common practice to represent a vector by a bold symbol $\mathbf{p}$ and its magnitude by the corresponding italic symbol p.

6.2 Aperture arrays in the shadow mask

The slots in the shadow mask of an ideal in-line-gun tube (Fig. 2a) are vertical and the effects of the bridging strips may be ignored, so the fundamental sampling frequency can be represented by a single horizontal vector. Ideally this is parallel to the line scan direction and at right angles to the vector representing the spatial frequency of the scan lines.

There are many possible ways of thinking of the shadow mask apertures of a delta-gun tube (Fig. 1) as being in an array of parallel straight lines, the four most obvious of them being shown in Fig. 8(a), and their spatial frequencies in the vector diagram Fig. 8(b). It can be seen from Fig. 8 that these four directions have their array lines inclined at ± 60° to the vertical (represented by $\mathbf{p}_r$ and $\mathbf{p}_s$ at ± 60° to the horizontal), horizontal (represented by the vector $\mathbf{p}_u$) and vertical (represented by the vector $\mathbf{p}_v$). The distance between adjacent apertures, for the tube used, was 0.68 mm from which:

$$p_r = p_s = p_v = 14.5 \text{ MHz}$$

$$p_u = 25.1 \text{ MHz}$$

From Fig. 8(b)

$$\mathbf{p}_u = \mathbf{p}_r - \mathbf{p}_s$$

$$\mathbf{p}_v = \mathbf{p}_r + \mathbf{p}_s$$

where the right-hand sides of the equations are a vector difference and a vector sum.

6.3 The sampling process

Sampling a pattern that is repetitive in one direction, with fundamental frequency f, but having no variation at right angles to that direction, by a shadow mask in which a set of parallel slots, which are parallel to the lines of the pattern, have a spatial frequency p has been shown (Section 5.1 and the Appendix) to result in alias components with frequencies $f_m = (mp \pm nf)$ where m and n are integers.

When the slots in the mask are not parallel to the lines of the pattern the spatial frequencies can be represented by vectors **p** and **f**. It is shown in the Appendix that the spatial frequencies of the alias patterns are now represented by the **vector** sums and differences ($m\mathbf{p} \pm n\mathbf{f}$). Particular cases with $m = 1$ are shown in Fig. 9.

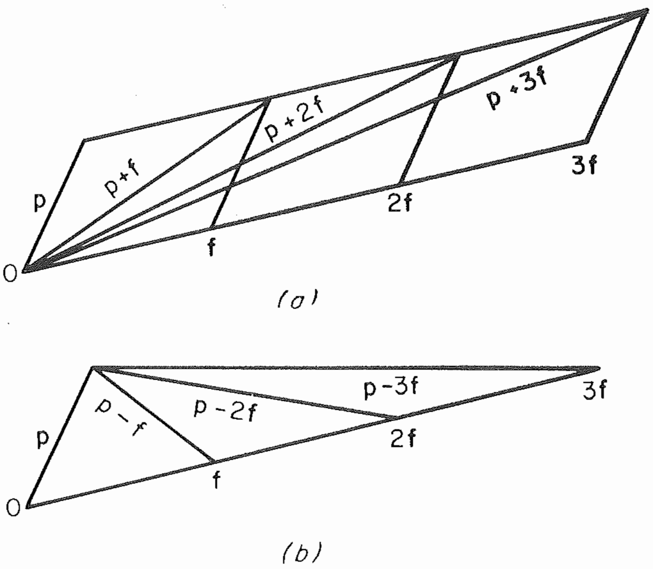

Fig. 9 - Vector sums and differences

(a) Vector sums of p with harmonics of f

(b) Vector differences between p and harmonics of f

A display may involve simultaneous sampling by two processes, such as the line structure of the raster represented by a vector $\mathbf{p}_L$ and the shadow-mask structure represented by a vector $\mathbf{p}_M$. The spatial frequencies of the alias components are represented by the vector sums and differences $(m_1\mathbf{p}_L \pm m_2\mathbf{p}_M \pm n\mathbf{f})$: if one of these is small the result is a moiré pattern.

6.4 A line-sweep signal displayed on a delta-gun tube

6.4.1 The display

Fig. 10 shows a display of the line-sweep signal on a 56 cm (22 in) delta-gun tube, with only the Green gun active. The sampling frequencies of the four principal ways in which the apertures may be thought of as forming arrays are given in Section 6.2 and the vertical sampling frequency of the lines of a field is

$$p_L = (4/3)\,(625-50)/(2 \times 52) = 7.37 \text{ MHz}$$

6.4.2 Sampling in the line direction only

The most prominent moiré patterning in Fig. 10 is produced by the apertures acting as vertical columns which are, to a close approximation, equivalent to vertical slots. The horizontal sampling frequency, represented in Fig. 8 by the vector $\mathbf{p}_v$, is 14.5 MHz (Section 6.1) and the resulting moiré patterns are centred on 14.5/2 = 7.25 MHz, 14.5/3 = 4.83 MHz and 14.5/4 = 3.62 MHz. The variations in the vertical direction of these moiré patterns, like those discussed in

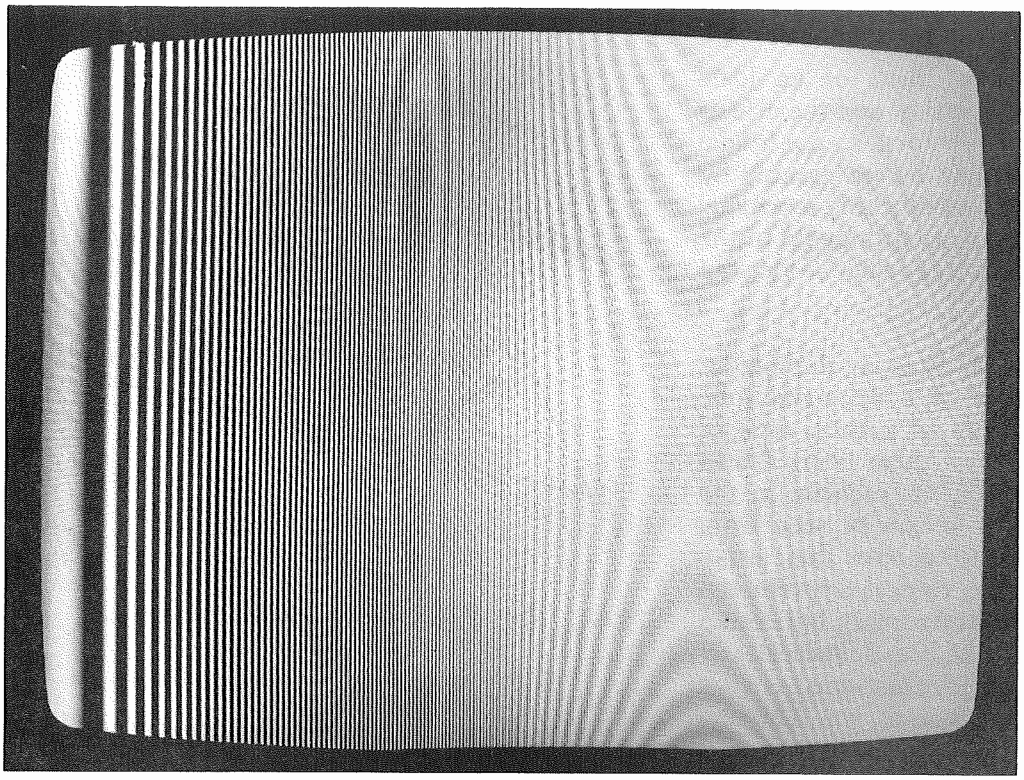

Fig. 10
Line-sweep waveform displayed on a delta-gun tube
(Green phosphor only)

Section 5.2 are caused by small variations in the display and/or in the shadow mask.

6.4.3 Sampling by the mask and the raster in the vertical direction only.

The bands visible at the sides of the display (Fig. 10), nearly horizontal across the middle of the screen and concave outwards towards the top and bottom, are examples of the interaction between the line raster and the apertures considered as rows, described in Section 3. The curvature of the dark bands shows that either the pattern of the apertures or the raster itself is not uniform, particularly towards the edges of the screen.

The spatial frequency of the lines of a field is 7.37 MHz (Section 6.4.1) while the vertical sampling frequency of the rows of dots, represented by the vector $\mathbf{p}_u$ in Fig. 8 is 25.1 MHz (Section 6.2). The moiré pattern would have a low spatial frequency if p_u were close to a harmonic of the line-raster frequency p_L, i.e. near to the condition $3p_L = p_u$ or $4p_L = p_u$. For minimum visibility, the optimum ratio would be $p_u/p_L = 3.5$, which compares closely with $25.1/7.37 = 3.4$ for this tube without overscan, slightly more if p_L is reduced by overscan.

Fig. 11 is an enlargement of the middle of the broad white band at the left hand side of Fig. 10. The beam focus of the tube is such that a scan line

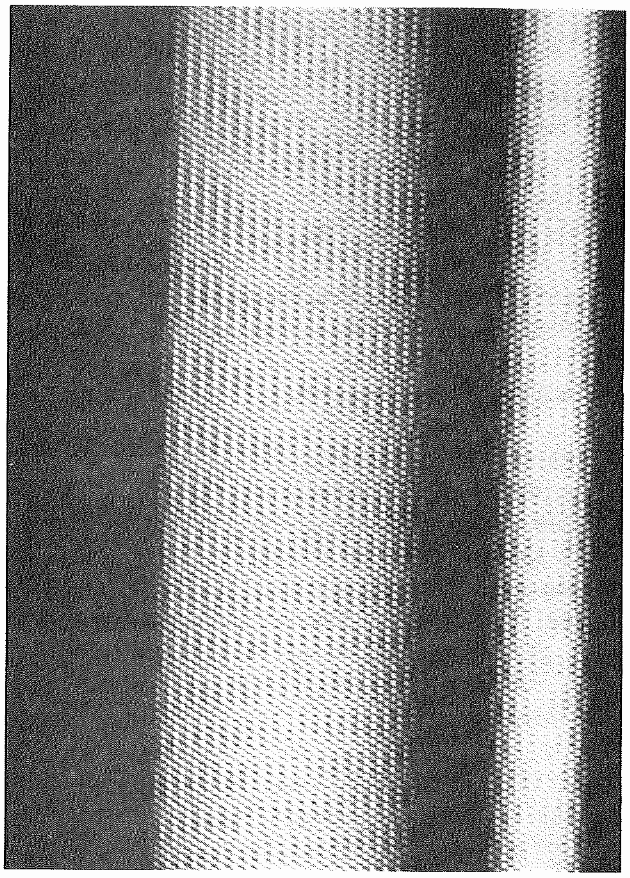

Fig. 11 - An enlargement of part of the left-hand note of Fig. 10.

that lies evenly between two horizontal rows of phosphor elements excites both of them, while a line that falls along the centre of a row of elements gives only slight excitation of the rows above and below. If the ratio of p_u to p_L were exactly 4 : 1 and the scan lines were the first type all the phosphor elements would be equally excited. However, if the lines were of the second type alternate rows of phosphor would be bright and the intermediate rows dim: because of the layout of the phosphors, this would result in alternate columns of phosphor being light and dark (these results are closely related to those discussed in Section 3). As was shown in the previous paragraph, in a practical condition the ratio p_u/p_L is chosen not to be integral and is probably not an exact ratio of small integers, so there is a continuous change from one condition to the other down the field scan, resulting in the patterning shown in Fig. 11.

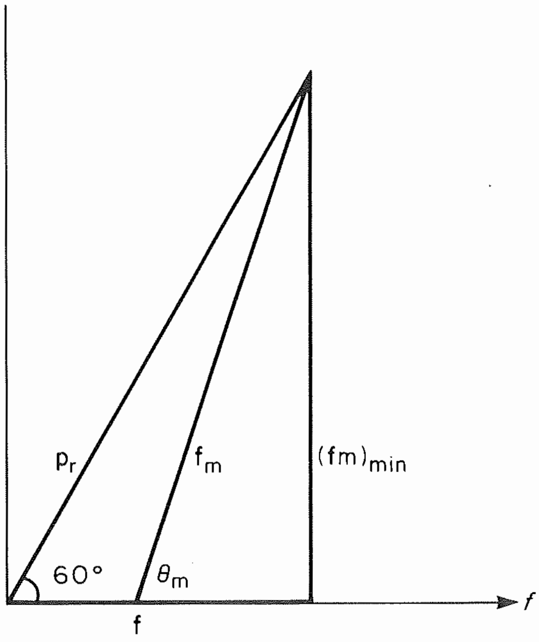

Fig. 12 - Vectors representing the sampling of a line-sweep signal by an oblique array of apertures.

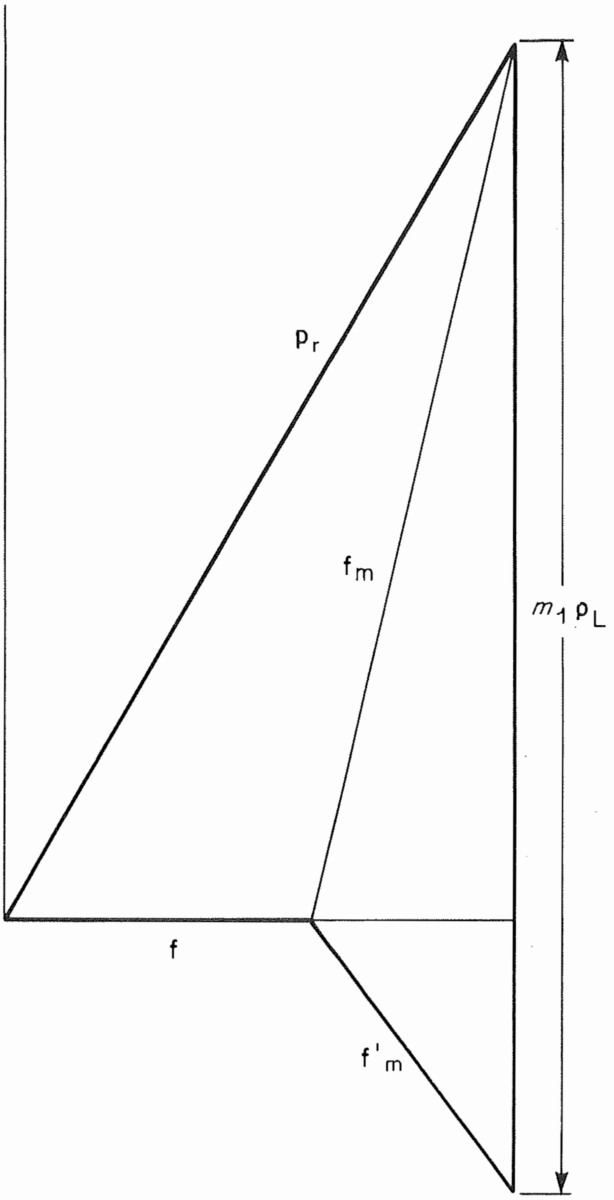

Fig. 13 - Vectors representing the simultaneous sampling of a line-sweep signal by an oblique array of apertures.

6.4.4 Sampling by the shadow mask in an oblique direction

The shadow mask apertures of a delta-gun tube, considered as oblique sampling arrays, may be represented by the vectors $\mathbf{p}_r$ and $\mathbf{p}_s$, as shown in Fig. 8 and discussed in Section 6.2. The vector $\mathbf{p}_r$ is shown again in Fig. 12., where the varying frequency of the line sweep waveform is represented by $\mathbf{f}$, with the alias frequency $\mathbf{f}_m$ given by the vector difference between $\mathbf{p}_r$ and $\mathbf{f}$. From the figure it is seen that $\mathbf{f}_m$ is smallest when it is at right-angles to $\mathbf{f}$, that its magnitude is then $(f_m)_{min} = p_r \sin 60° = 12.25$ MHz and that this minimum occurs when $f = p_r \cos 60° = 7.25$ MHz. (The same frequency as for the dominant moiré produced by horizontal sampling). The pattern frequency $(f_m)_{min}$ is too high for it to be visible, but it is made apparent by the sampling action of the raster. In Fig. 13 the vectors $\mathbf{p}_r$, $\mathbf{f}$ and $\mathbf{f}_m$ again represent the spatial frequencies of the mask, the sweep waveform and the alias component. In addition $m_1\mathbf{p}_L$ is a harmonic of the line frequency (cf. Section 6.3) producing an alias with spatial frequency $\mathbf{f}'_m$ which is the vector difference between $\mathbf{f}_m$ and $m_1\mathbf{p}_L$. Taking $m_1 = 2$, the minimum value of f'_m is $2p_L - (f_m)_{min} =$

$2 \times 7.37 - 12.25 = 2.49$ MHz. Consideration of the way in which $\mathbf{f'}_m$ varies in direction shows that the moiré pattern is curved and is convex upwards. Similar patterns, but convex downwards, result from simultaneous sampling by the mask, represented by $\mathbf{p}_s$, and the line scan. These are clearly seen in Fig. 10, although distorted by the irregularity in the mask or display that distorted the dominant moiré discussed in the previous section.

7. Reproduction of a hyperbolic zone plate test pattern

7.1 The test pattern

The properties of one particular form of hyperbolic zone plate pattern are described here: its basic principles and a way of generating it are considered in detail in Reference 3.

Ideally the pattern is rectangular with a 4 x 3 aspect ratio, and it is convenient to take an origin of co-ordinates at the top left corner, measuring x to the right and y downward. The luminance of the pattern varies sinusoidally, the horizontal component of the spatial frequency being constant along any horizontal line and proportional to y, the distance from the top, while down any vertical line the vertical component of the spatial frequency is constant and proportional to x, the distance from the left. The result can be written

$$v = \tfrac{1}{2}(1 + A \cos kxy)$$

where $A < 1$

and k is a constant.

The total spatial frequency at a point of the display has a magnitude proportional to the length of the line from the point to the origin of co-ordinates and has a direction that makes the same angle below the horizontal axis as the line makes to the right of the vertical axis.

A practical version which differs from this for instrumental reasons described in Ref. 3, is shown in Fig. 14 as displayed on a monochrome monitor. A typical feature is that the top, bottom and sides of the display are curved and the corners rounded, so it is not easy to locate the origin of the co-ordinates which is not actually on the display.

The dark band across the screen is centred on the horizontal line for which f_x is $3f_{sc}/2 = 6.65$ MHz, where f_{sc} is the PAL chrominance subcarrier frequency. Apart from the effects of field blanking the display is symmetrical about this line (which is slightly below the mid-height of the display), with f_x zero at the top, rising to 5.5 MHz at the edges of the dark band and falling to nearly zero again at the

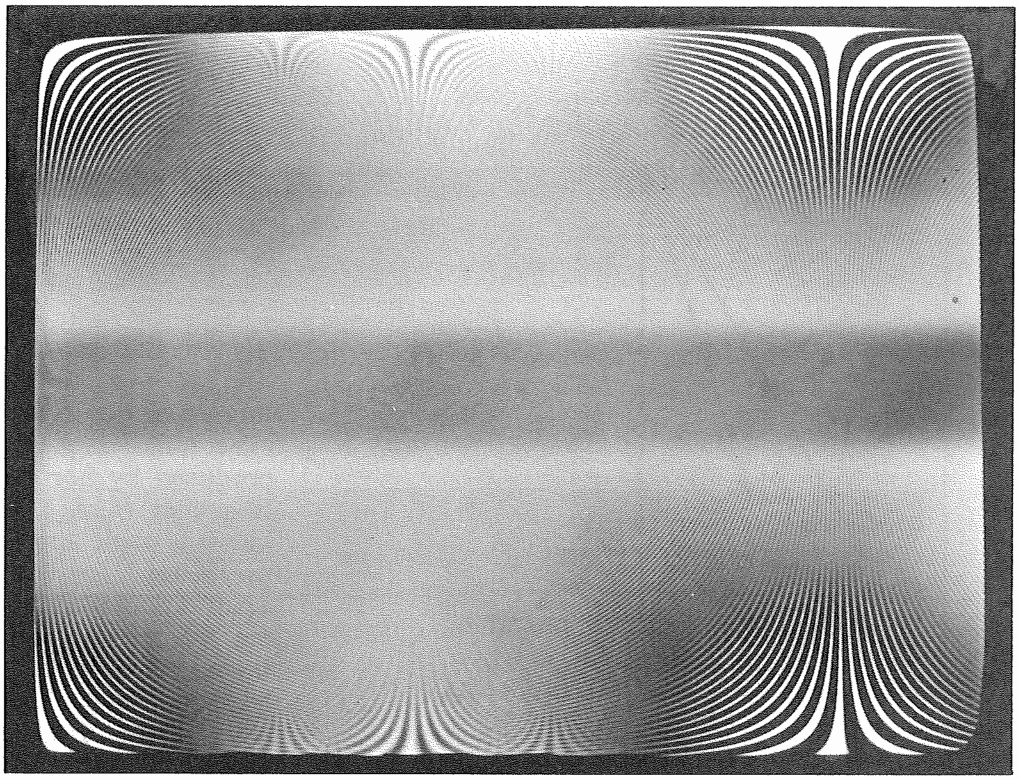

Fig. 14
Display of a hyperbolic zone plate test pattern on a monochrome tube.

bottom. Imperfections in the 5.5 MHz low-pass filter allow the transmission of our-of-band components that cause spurious patterning within the dark area. If either scan amplitude were changed the scale of the pattern would change, but not its shape. For example, taking a point (x_1, y_1) a known distance to the right of and below the origin, a reduction in the scan width in the ratio $q : 1$ increases the horizontal spatial frequency in the ratio $1 : q$. Also the vertical section of the pattern now at the point (x_1, y_1) was previously at the point (qx_1, y_1) so the change of scan amplitude also increases the magnitude of f_V at the point (x_1, y_1) in the ratio $1 : q$.

The major patterns on the top and bottom edges of the display, near the right-hand side, occur where the vertical spatial frequency of the zone plate is equal to $2p_L$ where p_L is the spatial frequency of the lines in a field. The other patterns, half way between each of them and the left-hand side occur where the vertical spatial frequency of the zone plate is p_L. Alternate fields carry dark and light lines and there is a marked 25 Hz flicker. The parts of the pattern where the contrast is greatest are very convenient for assessing the sharpness of focus of the scanning spot in the vertical direction.

Alias patterns can also be seen along the top and bottom edges where f_V is related to p_L in some simple way such as $f_V = p_L/2$, $3p_L/2$, $2p_L/3$ or $4p_L/3$, their visibility depending on the sharpness of focus (which in practice varies from point to point on the display).

7.2 The hyperbolic zone plate test pattern displayed on an in-line-gun tube

7.2.1 The display

The display of the pattern on an in-line-gun tube, with only the Green gun active, is shown in Fig. 15. The visibility of the moiré patterns depends critically on the sharpness of focus of the scanning beam: this was not uniform over the display so some are missing although their mirror-images in the axis of symmetry are apparent.

7.2.2 The moiré patterns

Apart from patterns at the top and bottom of the display, which are caused by the sampling action of the line raster alone and are discussed in the previous Section, and those on the left-hand edge which are caused by the slotted mask alone (the vertical component of spatial frequency of the zone plate being zero at $x = 0$), the moiré patterns seen in this display are the result of the combined sampling actions of the raster and the mask.

The major patterns lie on horizontal lines,

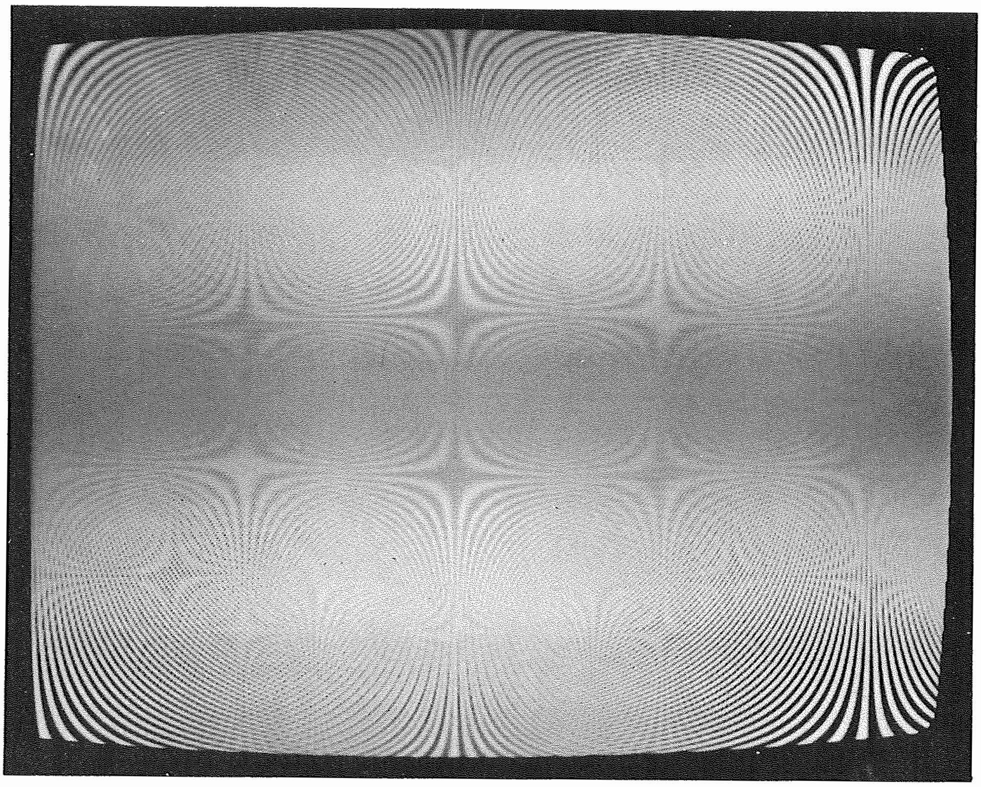

Fig. 15
Display of a hyperbolic zone plate test pattern on an in-line-gun tube

just outside the dark band, for which the horizontal component of spatial frequency of the hyperbolic zone plate f_x, is 5.3 MHz, i.e. one half of the sampling frequency of the mask, ($2f_x = p$ of Section 5.2) while other patterns can be seen on the lines for which $3f_x = p$ and $4f_x = p$. The positions of the patterns along the lines are those for which the vertical component of spatial frequency of the zone plate, f_y, is related to the spatial frequency of the lines of the field, p_L. The strongest patterns occur where $f_y = 2p_L$, $2f_y = p_L$, $2f_y = 3p_L$ and weak patterns at $f_y = p_L/3$, $2p_L/3$ $4p_L/3$ and $5p_L/3$ in the bottom part of the display (but not where $f_y = p_L/2$ or p_L although each of these would probably be visible if it were the only pattern on the display).

7.3 The hyperbolic zone plate test pattern displayed on a delta-gun tube

7.3.1 The display

The display on a delta-gun tube, with only the Green gun active, is shown in Fig. 16. The discussion in Section 6.4 has shown that the sampling of the raster by the shadow mask is not precisely according to the ideal pattern: the combination of this with the curvature of the picture edges, the rounding of the corners and the slight overscan of the screen leads to discrepancies between the actual and predicted positions of the moiré patterns up to about 5% of picture height.

7.3.2 The moiré patterns

Apart from the patterns at the top and bottom of the display, caused by the line scan raster alone as discussed in Section 7.1, there are four main moiré patterns, symmetrically placed about the vertical line corresponding to the vertical spatial frequency $f_y = p_L$. The visibilities of the minor patterns depend critically on the adjustments of the focus and brightness controls of the monitor and they tend to be less apparent on a photograph than when viewed directly on the monitor.

The top left of the four main moiré patterns is on a line from the top left corner of the display (allowing for overscan) at 30° below the horizontal, i.e. the spatial frequency of the zone plate is at an angle of 60° with the horizontal (Section 7.1). This corresponds to the direction of the $\mathbf{p}_s$ vector representing the arrays of apertures (Fig. 8b) whose magnitude is 14.5 MHz and whose horizontal and vertical components are 7.25 MHz and 12.55 MHz respectively. Estimation of the position of the moiré relative to the dark band and to the vertical line where the vertical component of zone plate frequency, f_y, is equal to p_L, confirms that the moire corresponds to the condition $2\mathbf{f} = \mathbf{p}_s$ and the magnitude of $\mathbf{f}$ is 7.25 MHz. The vestigial pattern in the dark bar just to the left of the line

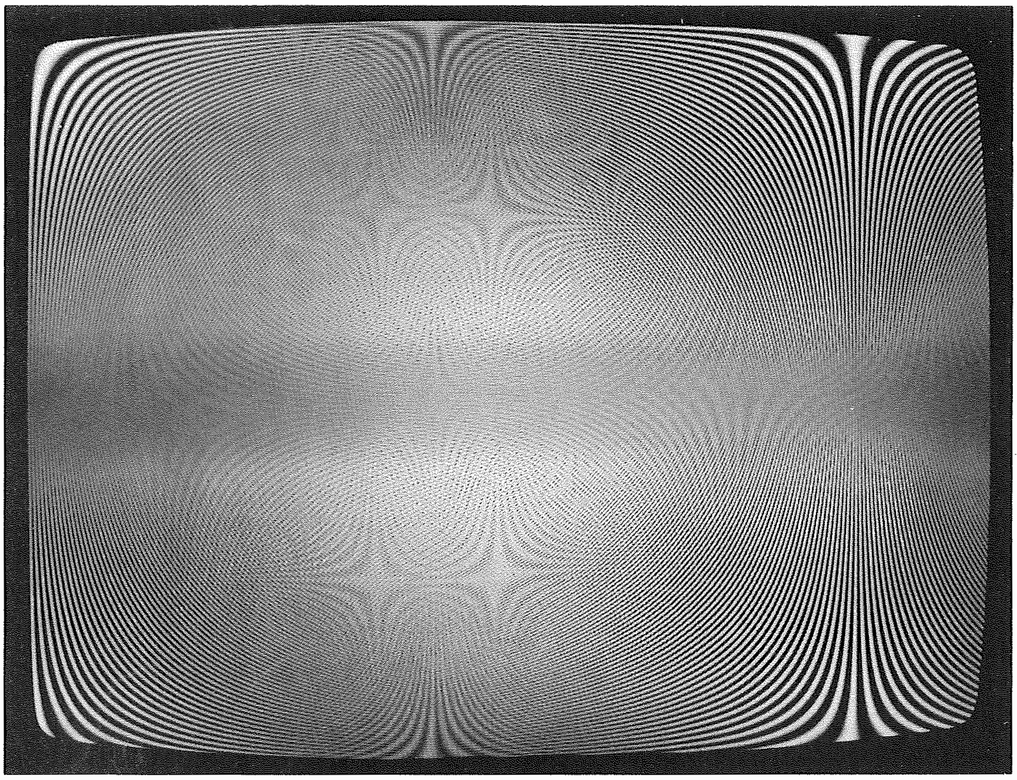

Fig. 16
Display of a hyperbolic zone plate test pattern on a delta-gun tube

corresponding to $f_y = 2p_L$ and on the straight line from the corner of the display through the main moiré shows that if the mask pattern were coarser the moiré corresponding to $\mathbf{f} = \mathbf{p}_s$ could be visible. This can be simulated by reducing the horizontal scan amplitude of the display (Section 7.1).

Similarly, the bottom left moiré of this set corresponds to the condition $2\mathbf{f} = \mathbf{p}_r$, the spatial frequency of the pattern being at 30° above the horizontal. At the position of the top right moiré of the set the horizontal component of spatial frequency of the zone plate is the same as for the other two patterns, but the vertical component is the difference between $2p_L$ and the vertical component of the other two. Bearing in mind the relative magnitudes of the components, it is seen that this moiré corresponds to the condition $2\mathbf{f} = \mathbf{p}_r + 4\mathbf{p}_L$ (where $\mathbf{p}_L$ is directed down-

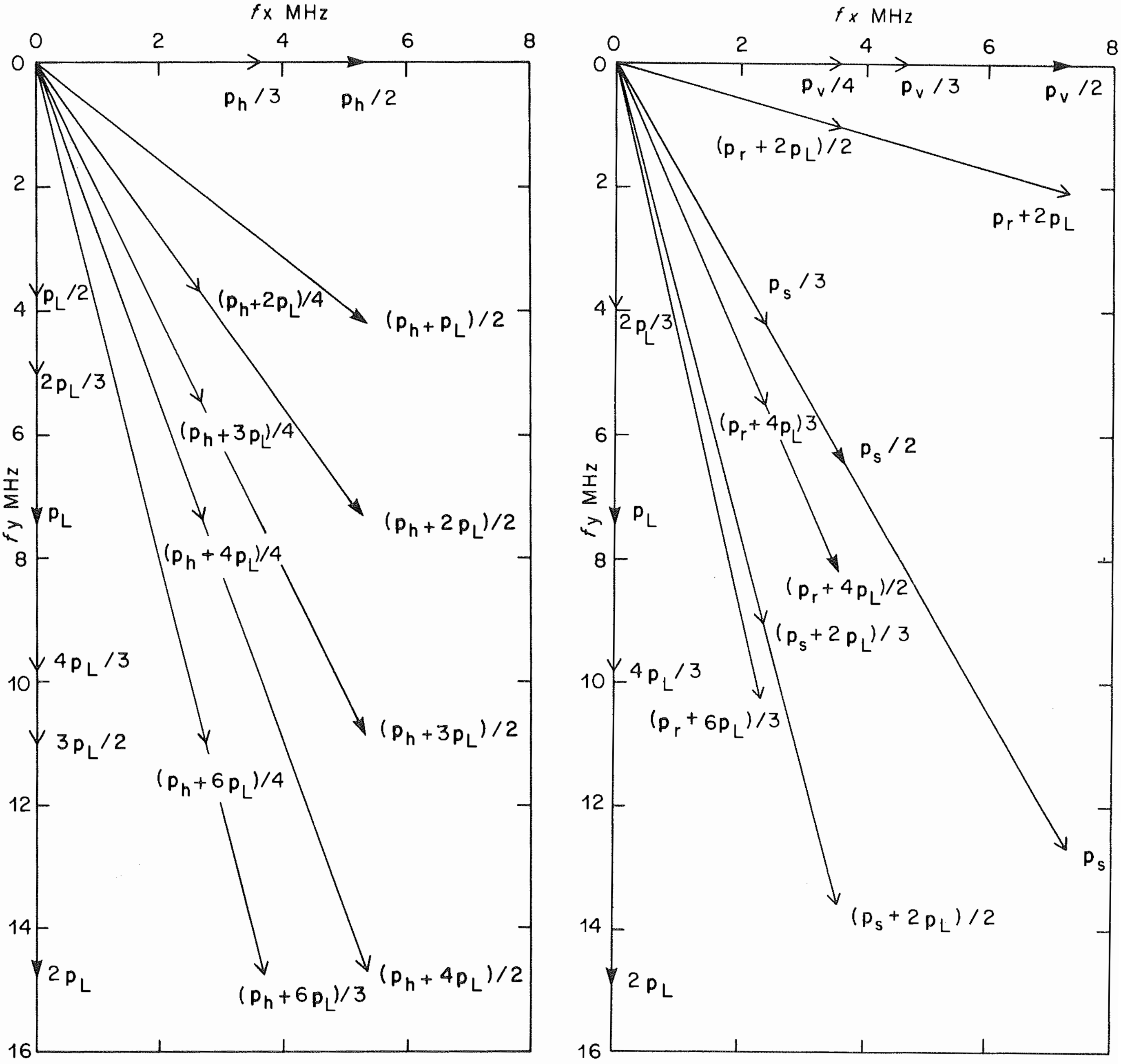

(a) *(b)*

Fig. 17 - Vector representations of repetitive patterns that can cause moiré patterns (one quadrant only)

(a) in-line-gun tube (b) delta-gun tube

⟶ Major patterns ⟶ Minor patterns

wards) and the magnitude of *f* is

$$\left\{[7.25/2]^2 + [(2 \times 7.37) - (12.55/2)]^2\right\}^{1/2} = 9.21 \text{ MHz}.$$

Similarly, the bottom right of the four main moirés is represented by $2\mathbf{f} = \mathbf{p}_s - 4\mathbf{p}_L$.

Minor patterns that can be seen on the display, although they are considerably less conspicuous than the four considered above, include

(a) patterns at the same horizontal levels as those already considered, again involving the relationship between $2\mathbf{f}$ and $\mathbf{p}_r$ or $\mathbf{p}_s$ but different harmonics of $\mathbf{p}_L$.

(b) patterns on the lines parallel to those considered in (a), but two thirds of the way to the levels at which the horizontal spatial frequency is zero, corresponding to relationships involving $3\mathbf{f}$, $\mathbf{p}_r$ or $\mathbf{p}_s$ and harmonics of $\mathbf{p}_L$.

8. Conclusions

The shadow mask and phosphor layout of a shadow mask colour television tube impose onto the display a sampling process in addition to that resulting from the line structure of the raster. Two forms of tube are in current use, one with the guns clustered round the tube axis and a shadow mask with circular holes in a honeycomb pattern, the other with guns in a horizontal plane and a mask with vertical slots. Although the latter form of mask has marginally the higher transparency, considerations of mechanical rigidity allow the former to have the finer construction and therefore the better horizontal resolution. The biggest part of the price paid for this is that the mask of a delta-gun tube has a significant sampling action in the field-scan direction which can interact with the raster line structure.

Sampling effects involving repetitive patterns can be described in terms of vectors that represent the spatial frequencies involved. Figs. 17 (a) and (b) show, in vector form, those spatial frequencies that can produce moiré patterns on in-line-gun and delta-gun tubes respectively, the frequency scales referring to representative current 56 cm (22 in) tubes.

Manufacturers appear, at present, to produce delta-gun tubes with dot-phosphor screens that have higher resolution than the corresponding in-line-gun tubes with stripe-phosphor screens. This militates against the use of in-line-gun tubes in applications where resolution or close viewing is important. An interesting possibility would be the use of a dot-phosphor screen with an in-line-gun assembly, combining the resolution of the former with the simpler convergence and purity controls of the latter.

9. References

1. REED, C.R.G. Two colour television tubes with precision in-line-gun assemblies. BBC Research Department Report No. 1977/13.

2. WRIGHT, W.W. Recent developments in shadow mask tubes for colour television. Royal Television Society Journal, **13**, 10, July/August 1971, pp. 221 – 230.

3. DREWERY, J.O. The zone plate as a television test pattern. BBC Research Department Report No. 1978/23.

4. BIBERMAN, L.B. (Editor). Perception of displayed information. Plenum Press, New York & London, 1973, Chapter 7.

5. BRACEWELL, R. The Fourier Transform and its applications. McGraw Hill, 1965.

6. PETERSEN, D.P. *and* MIDDLETON, D. Sampling and reconstruction of wave-number limited functions in N-dimensional Euclidean spaces. Information + Control, **5**, pp. 279 – 323 (1962).

10. Appendix

The sampling of repetitive patterns

10.1 Introduction

This Appendix considers the processes involved in the sampling of repetitive patterns displayed on a shadow-mask colour television tube. The treatment is simplified by the omission of a considerable amount of detail that could add to the mathematical rigour or could illustrate the finer points of the processes involved, but it is sufficient to account for the more important effects seen on a display. In particular, only stationary patterns are considered.

For the purposes of this Report, a repetitive pattern is one in which the part of the display which is of particular interest is occupied by straight parallel bars that have no variation along their length but at right-angles to this the luminance variation is, for all practical purposes, repetitive for a few cycles. The distance between wave-crests, at right-angles to the length of the bars, is the wavelength λ mm and the spatial frequency is $p = 1/\lambda$ cycles/mm or, more conveniently, $W/52\lambda$ MHz where W is the display width.

The pattern outside the area of particular interest may be different from the sum of the terms of the spectrum (which continues repeating the pattern): it does not even exist beyond the edge of the tube face. Care must therefore be taken not to push the results beyond the conditions for which they are valid.

10.2 Spectral components

Repetitive vertical bars can be represented by a function $g(x)$ which is independent of the vertical co-ordinate y but varies repetitively with x over the region of interest. Provided the origin of co-ordinates lies at least half a wavelength from each side of this region $g(x)$ can be represented (using simple Fourier Analysis) by the sum of the terms:

$$a_0 + a_1 \cos 2\pi p x + a_2 \cos 4\pi p x + \ldots\ldots$$

$$+ a_n \cos 2 n \pi p x + \ldots\ldots \text{etc.}$$

$$+ b_1 \sin 2 \pi p x + b_2 \sin 4 \pi p x + \ldots\ldots$$

$$+ b_n \sin 2 n \pi p x + \ldots\ldots \text{etc.}$$

where
$$a_0 = \frac{1}{X}\int_{-X/2}^{X/2} g(x)\,dx$$

$$a_n = \frac{2}{X}\int_{-X/2}^{X/2} g(x) \cos 2\pi n p x\,dx$$

and
$$b_n = \frac{2}{X}\int_{-X/2}^{X/2} g(x) \sin 2\pi n p x\,dx \qquad (1)$$

Alternatively, the spectrum could be written:

$$g(x) = a_0 + c_1 \cos(2\pi p x - \phi_1) + \ldots\ldots$$

$$c_n \cos(2n\pi p x - \phi_n) + \ldots\ldots \text{etc.}$$

where $c_n = \sqrt{(a_n^2 + b_n^2)}$ (taking the positive root)

$$\tan\phi_n = b_n/a_n$$

$$\cos\phi_n = a_n/c_n$$

$$\sin\phi_n = b_n/c_n \qquad (2)$$

If the pattern is rotated so that the repetitive bars are oblique to the axes it can easily be shown that the spatial frequencies in the x and y directions are:

$p_x = p \cos\theta$

$p_y = p \sin\theta$ where θ is the angle of rotation

from which

$p^2 = p_x{}^2 + p_y{}^2$

or $1/\lambda^2 = 1/\lambda_x^2 + 1/\lambda_y^2$

where λ_x, λ_y are the wavelengths measured along the x and y axes (3)

The spectrum of the waveform can be written as the sum of a constant term a_0 and sinusoidal terms in cos $2\pi\ (p_x x + p_y y)$, sin $2\pi\ (p_x x + p_y y)$ and their harmonics.

The spatial frequencies of the components of such a pattern can be represented in magnitude and direction by vectors, all in the same direction, with the lengths of those representing the harmonics equal to integral multiples of that representing the fundamental.

The signs of the vectors are not given any significance in the Report. On the other hand the pattern has characteristics that are not represented by the vectors, in particular the amplitudes and phases of the spectral components which affect the visibility of the spurious patterns produced by sampling but do not affect their spatial frequencies. More complicated notations could be used that cover these factors and can be generalised to include other patterns, but they are beyond the needs of the present Report. Some aspects of the problem are considered in more detail in References 4, 5, and 6.

10.3 One-dimensional sampling

Consider a monochrome display tube, having a single electron gun and a continuous uniform phosphor, without a shadow mask. Under normal scan conditions the display is controlled by the signal applied to the electron gun but is modified by several factors which include the sharpness of focus of the electron beam, the linearity of the scan raster (including the effects of pincushion distortion and its correction) and flare in the faceplate. If a shadow mask were inserted into the tube, at a potential that did not disturb the scan characteristics, only parts of the phosphor would be excited but their brightness would be virtually unchanged. The small differences would be caused by a reduction in the flare from the surrounding phosphor: however, in a three-colour tube, there would be partial compensation from the flare from the adjacent phosphor areas of the other colours. It is thus a close approximation to say that if the unsampled display and the sampling action were each the same on every line the action could be represented by:

$$i(x) = s(x)\ .\ v(x)$$

where $i(x)$ is the luminance after sampling

$s(x)$ represents the sampling process

$v(x)$ is the luminance that would have been produced in the absence of sampling, all of which vary with x but are independent of y.

In a region over which $s\ (x)$ and $v\ (x)$ are repetitive, in the sense understood in Section 10.1, each of them may be represented by a spectrum, through the two spectra have different fundamental spatial frequencies. From Equations (3) we can write

$$\begin{aligned} v\ (x) = c_0 &+ c_1 \cos (2\pi f x - \phi_1) \\ &+ c_2 \cos (4\pi f x - \phi_2) + \text{......etc} \\ &+ c_n \cos (2\pi\, n f x - \phi_n) + \text{....etc} \\ s(x) = d_0 &+ d_1 \cos (2\pi p\, x - \psi_1) \\ &+ d_2 \cos (4\pi p\, x - \psi_2) + \text{........} \\ \text{..............} &+ d_m \cos (2\pi\, m\, p\, x - \psi_m) + \end{aligned} \tag{4}$$

From the product $i(x) = s\ (x)\ .\ v\ (x)$ it is seen that i(x) has four types of component (which were collected into two groups in Section 5.1).

(1) a d.c. term

(2) the components of the original display $v\ (x)$ multiplied by d_0 the mean transmission of the sampling system

(3) the components of the sampling pattern $s\ (x)$ multiplied by c_0 the mean luminance of the original display.

(4) components represented by the typical product:

$$d_m \cos (2\pi\ m\ p\ x - \psi_m)\ .\ c_n \cos (2\ \pi\, n\, f x - \phi_n)$$

Multiplying out the term (4) gives two components

$$\begin{aligned} &\tfrac{1}{2} c_n d_m \cos\ [2\pi\ (mp + nf)_x - (\psi_m + \phi_n)] \\ \text{and } &\tfrac{1}{2} c_n d_m \cos\ [2\pi\ (mp - nf)_x - (\psi_m - \phi_n)] \end{aligned} \tag{6}$$

This pair of terms can be thought of as sidebands separated from the sampling waveform component *mp* by plus or minus the display component, *nf*, unless *nf* is greater than *mp*, when the second of the terms may be written (remembering that, for any angle θ, cos $[-\theta]$ = cos $[\theta]$),

$$\tfrac{1}{2} c_0 d_0 \cos\ [2\pi\ (nf - mp)\, x - (\theta_n - \psi_m)]$$

and the two terms can be thought of as sidebands spaced ± *mp* about the display component *nf*.

When a pattern is moved without changing its shape all of its spatial frequency components move through the same distance. In the representation of $v\ (x)$ in Equation (5) for example, this could be represented by replacing x by $(x + x')$ where x' is the distance moved. Alternatively, if the fundamental component is represented as changing through a phase angle ϕ', where $\phi' = 2\pi f x'$, it becomes $c_1 \cos\ [2\pi\ f\ x\ -\ (\phi\ -\ \phi')]$ and the representative component becomes

$$c_n \cos\ [2\pi\, n\, f x - (\phi_n - n\phi')]\,.$$

If there is also a local displacement of the sampling pattern, $s(x)$, equivalent to a phase change ψ' in its fundamental component, the sampled components corresponding to Equation 6 become:

$$\tfrac{1}{2} c_0 d_0 \cos\ [2\pi\,(mp \pm nf)\,x - \ (\psi_m - m\psi') \pm (\phi_n - n\phi')\ ]\,.$$

This was stated, in a simplified form, in Section 5.1.

10.4 Two-dimensional sampling

Two-dimensional sampling is involved when either (or both) of the unsampled display and the sampling pattern is rotated, as considered in the second half of Section 10.2, (with the trivial exception of the case where they are rotated equally). From that Section, a typical spectral component of the unsampled display can be written as:

$$c_n \cos\ [2\pi n\ (f_x x + f_y y) - \phi_n]$$

where the total spatial frequency is given by

$$f = \sqrt{(f_x{}^2 + f_y{}^2)}$$

and the angle of rotation θ_f by $\sin\theta_f = f_y/f$

$$\cos\theta_f = f_x/f$$

$$\tan\theta_f = f_y/f_x$$

Similarly, a typical spectral component of the sampling pattern can be written as

$$d_m \cos\ [2\pi\, m\ (p_x x + p_y y) - \psi_m]$$

The theory follows that of Section 10.3, the spectral components of the display after sampling, equivalent to (4) of that Section, being represented by the product

$$d_m \cos\ [2\pi m(p_x x + p_y y) - \psi_m]$$
$$\text{x}\ c_n \cos\ [2\pi n(f_x x + f_y y) - \phi_n]$$

Multiplying these gives the spectral components

$$\tfrac{1}{2}\, c_n d_m \cos\ [2\pi\ (mp_x + nf_x)\,x + + (mp_y + nf_y)y\ - (\psi_m + \phi_n)]$$

and

$$\tfrac{1}{2}\, c_n d_m \cos\ [2\pi\ (mp_x - nf_x)\,x + +(mp_y - nf_y)y\ - (\psi_m - \phi_n)]$$

These represent repetitive patterns whose spatial frequencies, like those of the c_n and d_m terms producing them, can be represented by vectors. The x terms of the spatial frequencies are the sum and difference of the x terms of the components producing them, and similarly for the y terms. The vectors representing the resulting patterns are therefore the vector sum and difference of the vectors representing the components producing them, i.e. if $\mathbf{f}_m$ is the vector representing one of these patterns and $m\mathbf{p}$ and $n\mathbf{f}$ are the vectors representing the components producing them:

$$\mathbf{f}_m = m\mathbf{p} \pm n\mathbf{f}$$

10.5 The sampling effects of a shadow mask

The slots in the mask of an in-line-gun tube can be treated, to a very close approximation, as though they were continuous and the spatial frequency represented by a vector at right-angles to them. The slots in a practical tube are bridged, as shown in Fig. 2, the bridges being in arrays at approximately ± 45° to the vertical. Their effects on the sampling process can be represented by vectors at approximately ± 45° to the horizontal, but the bridges are usually so thin that their effects can be ignored.

The apertures in the mask of a delta-gun tube can be treated as being arranged in two sets of arrays, at ± 60° to the vertical each of which samples the other to produce, inter alia, horizontal and vertical arrays of apertures (Fig. 8). The theory developed in this Report does not consider the numerical effects of the shape and size of the apertures, nor of the sharpness of focus of the scanning beams.

CJS/VY

Printed by BBC RESEARCH DEPARTMENT, Kingswood Warren, Tadworth, Surrey, KT20 6NP